Triply Periodic Minimal Surfaces: An Overview of Their Features, Failure Mechanisms, and Applications

Arpit Gupta* and Sunith Babu L

Department of Mechanical Engineering, M S Ramaiah Institute of Technology Bangalore, India. *E-mail: Guptaarpit175@gmail.com

Abstract

Additive manufacturing has made it possible to create complicated geometries and lattice structures, and it is also the greatest approach for producing nature-inspired cellular structures. Triply periodic minimal surface (TPMS) cellular structure, which is additively built, has a high strength-to-weight ratio, making it useful in various applications, including structural weight reduction, biomedical, aerospace, and impact absorption. TPMS is a natural-inspired surface with zero mean curvature and a local minimal area. The type of structure, loading mechanism, unit cell characteristics, and relative density significantly affect the structure's strength and stiffness. As a result, this article will cover the history, classification, characteristics, manufacturing processes, failure mechanism, and applications of the TPMS.

Keywords: TPMS, cellular structures, gyroid, primitive, additive manufacturing

1.0 Introduction

Almost all engineering applications require high energy characteristics to minimize the extent of the damage. The cellular structure comprises randomly or periodically arranged microstructures that are inspired by nature. The microstructure of bone which has low density and yet offers high strength and stiffness is an example of cellular structure, beetle shells, butterfly wings, and sea urchins are some more natural examples of cellular structures that exhibit high strength to weight ratio. Figure 1 shows the examples of TPMS cellular structure in the C. Rubi butterfly wings (Al-Ketan and Abu Al-Rub, 2019; Lai et al., 2007; Poladian et al., 2008; Sharma and Hiremath, 2021). Because of the high strength to weight ratio and outstanding energy absorption feature, the cellular structure has grabbed the attention of researchers as they are the best candidate for prosthetics,

bioscaffolds, tissue engineering, battery electrode, etc (Tafazoli and Nouri, 2020).

As a result, in 1925 first attempt was made to synthesize cellular materials by a process that embodies voids in metals. Many cellular structures exist in foam and lattice types in today's world. Foam types of cellular materials are used for high energy absorption, stiffness, and strength-related applications. Whereas lattice cellular structure is used in events where more control over the deformation is needed (Sharma and Hiremath, 2021).

The three most common lattice structures are struct, planar and surface-based lattice. The struct-based lattice structure (Figure 2(a) is constructed by connecting a series of rod-like forms in various orientations to form a unit cell.The planar-based lattice structure (Figure 2(b) is created by extruding a 2D plane in a single direction.

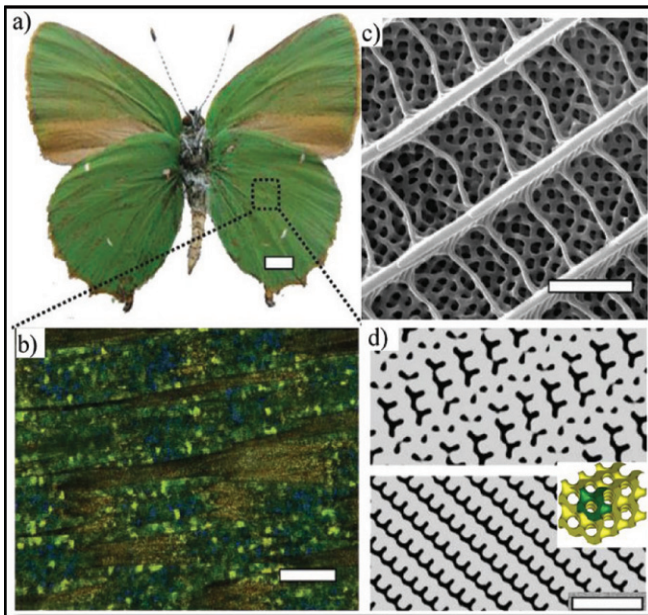A trigonometric equation is used to generate a surface-

Figure 1: (a) Image of c. Rubi butterfly, (b) and (c) Image of gyroid structure present on wings, (d) SEM image of the structure (Tafazoli & Nouri, 2020)
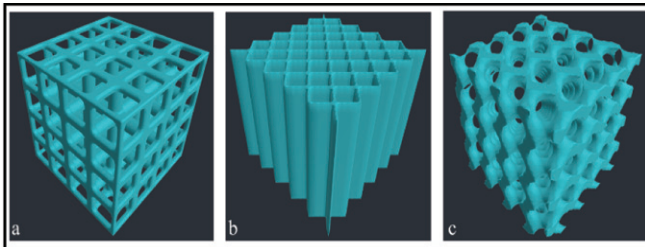

Figure 2: (a) Struct-based lattice, (b) Planar-based lattice, (c) Surface-based lattice

based lattice (Figure 2(c) these equations can be modified to control the size, shape, and density of a unit cell.

A triply periodic minimal surface (TPMS) is a subset of the surface-based lattice. TPMS are of two types: sheet-based and skeletal-based surface lattice shown in Figures 3 and 4 respectively. Skeletal-based lattice can be used for bioscaffolds and sheet-based lattice can be used in thermal management applications due to its higher surface area to volume ratio (Feng Lu et al., 2018; L. Wang et al., 2011; Yan et al., 2014). Until recently, fabricating cellular lattices with complicated geometry was a tough operation due to the shrinking size factor. However, new advancements in additive manufacturing technology have aided in the construction of intricate microcellular structures (Frazier, 2014; Guo and Leu, 2013a).

2.0 Triply Periodic Minimal Surface

In 1865, Schwarz described the first TPMS, and in 1883, his pupil E.R. NEOVIUS produced four more TPMS (Schwarz, 2005). ALAN SCHOEN created 12 more TPMS in the year 1970. Figure 5 depicts some of the TPMSs.

A TPMS has the smallest area for a given boundary because it has a local minimal area and zero mean curvature. Soap film is an example of TPMS in which surface tension reduces surface area (H. Y. Chen et al., 2009; Torquato and Donev, 2004). TPMS surfaces are approximated using mathematical equations, such as the Fourier series presented in equation (1), which can be changed to manage cell shape, size, and density.

$$\varphi_{(r)} = \sum_k F(k)\cos\left(2\pi kr - \alpha(k)\right) \qquad \dots (1)$$

Where "k are the reciprocal vectors, structure factor $f(k)$ is an amplitude associated with a given k-vector, and $\propto (k)$ is
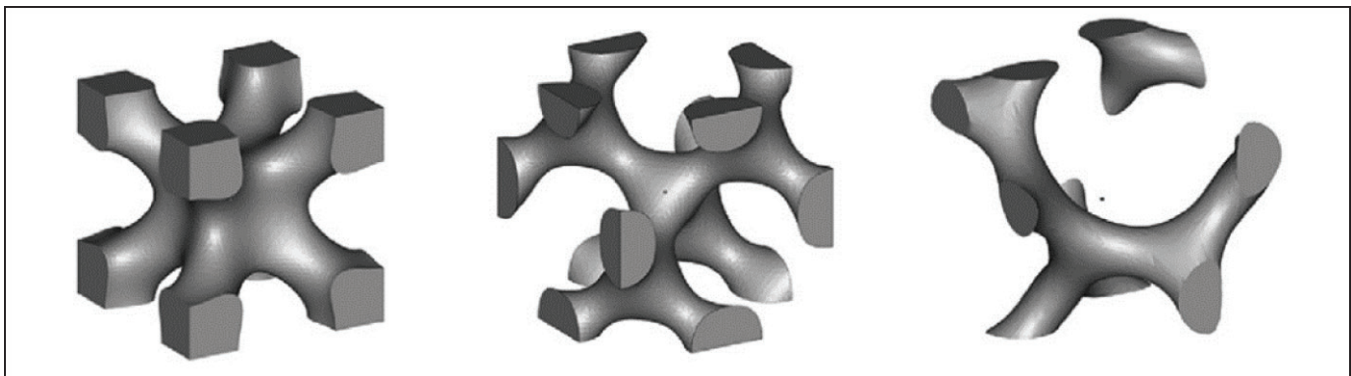

Figure 3: Skeletal IWP, skeletal diamond, skeletal gyroid- TPMS cellular structure (Al-Ketan et al., 2018)
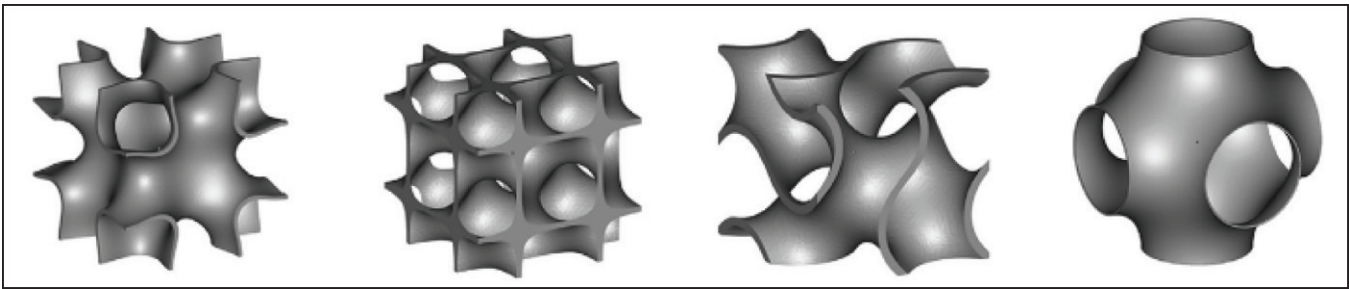
Figure 4: Sheet IWP, sheet diamond, sheet gyroid, sheet primitive- TPMS cellular structure (Al-Ketan et al., 2018)
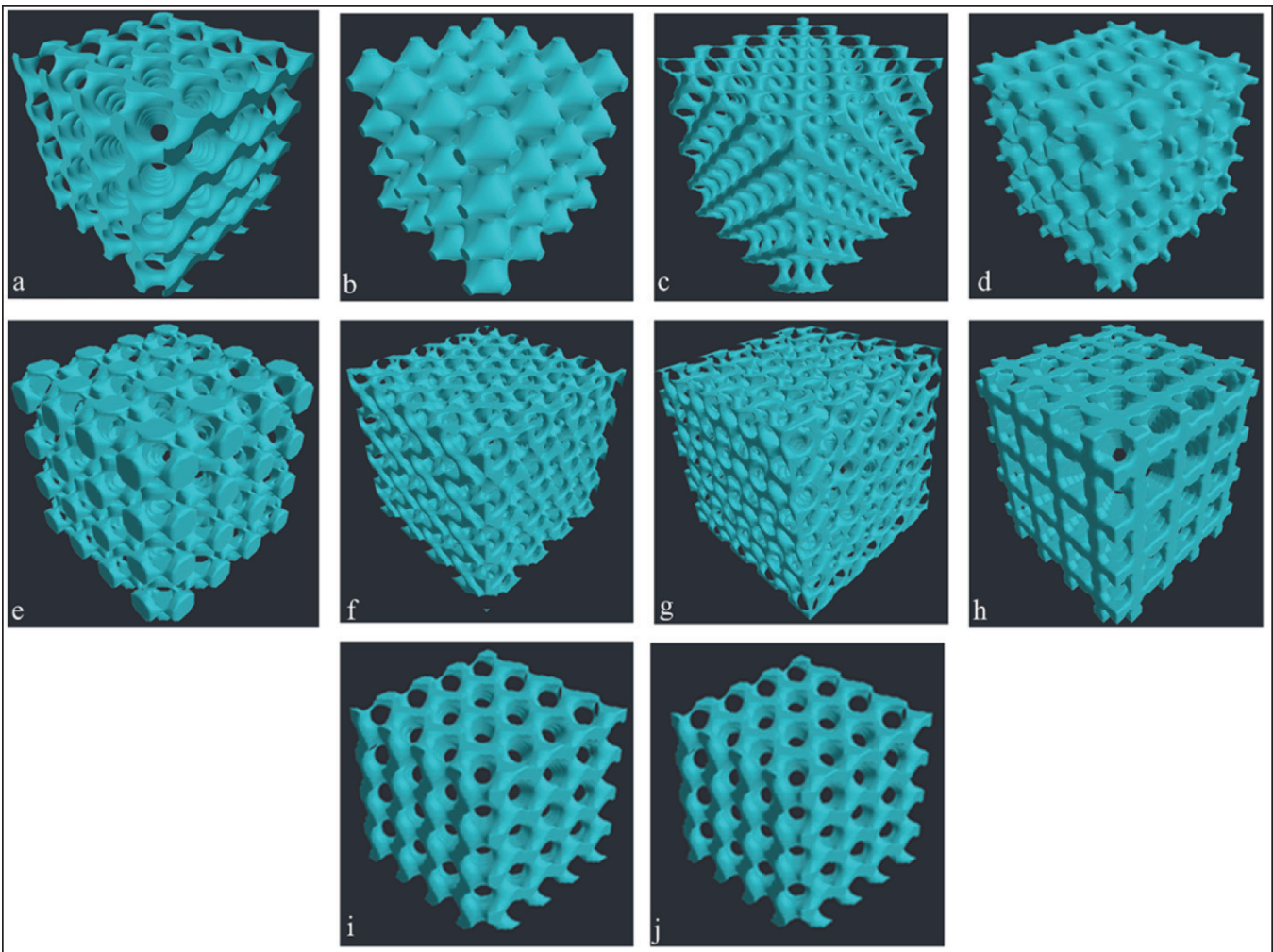

Figure 5: Various TPMS structures developed using GEN3D software (a) Gyroid, (b) Schwarz P, (c) Schwarz D, (d) Neovius, (e) Primary IWP, (f) Fischer Koch, (g) Split P, (h) Secondary IWP, (i) Scherk First, (j) Scherk Second

a phase shift" (Gandy and Klinowski, 2002). Some of the most familiar TPMS with their approximate equations are mentioned below:

Schwarz Primitive

$$\Phi_P = cosx + cosy + cosz = c \qquad \dots (2)$$

(Infinite Periodic Minimal Surfaces without Self-Intersections - NASA Technical Reports Server (NTRS), n.d. –a)

Schoen Gyroid

$$\Phi_G = sinx\ cosy + siny\ cosz + sinz\ cosx = c \qquad \dots (3)$$

(Infinite Periodic Minimal Surfaces without Self-Intersections - NASA Technical Reports Server (NTRS), n.d. – a)

Schwarz Diamond

$$\Phi_D = \text{cosx cosy cosz} - \text{sinx siny sinz} = c \qquad \text{... (4)}$$

(Infinite Periodic Minimal Surfaces without Self-Intersections - NASA Technical Reports Server (NTRS), n.d. – a)

Schoen -IWP

$$\Phi_{IWP} = 2(\text{cosx cosy} + \text{cosy cosz} + \text{cosz cosx})$$
$$- (\text{cos2x} + \text{cos2y} + \text{cos2z}) = c \qquad \text{... (5)}$$

(H. Chen et al., 2020)

Fischer-Koch S

$$\Phi_s = \text{cos2x siny cosz} + \text{cosx cos2y sinz}$$
$$+ \text{sinx cosy cos2z} = c \qquad \text{... (6)}$$

(H. Chen et al., 2020)

Schoen -FRD

$$\Phi_{FRD} = 4(\text{cosx cosy cosz}) -$$
$$(\text{cos2x cos2y} + \text{cos2y cos2z} + \text{cos2z cos2x}) = c \qquad \text{... (7)}$$

(H. Chen et al., 2020)

Schwarz- Neovius

$$\Phi_N = 3(\text{cosx} + \text{cosxy} + \text{cosz}) + 4(\text{cosx cosy cosz}) = c \quad \text{...(8)}$$

(H. Chen et al., 2020)

Where $x = \frac{2\pi X}{L_x}$, $y = \frac{2\pi Y}{L_y}$, $z = \frac{2\pi Z}{L_z}$ and L_x, L_y, L_z are the size of the unit cell in the X, Y, and Z-direction (H. Chen et al., 2020; Infinite Periodic Minimal Surfaces without Self-Intersections - NASA Technical Reports Server (NTRS), n.d. – b)

3.0 Mechanical Properties

This section gives a brief idea about the standards to be followed to carry out the mechanical testing of the cellular components, the general failure models, properties, and factors that affect these properties.

Due to a lack of criteria for assessing additively manufactured cellular structures, ISO 13314:2011 is widely recommended. It was intended to evaluate materials having randomly oriented voids, but it is equally applicable to additively form cellular structures (ISO - ISO 13314:2011 - Mechanical Testing of Metals – Ductility Testing – Compression Test for Porous and Cellular Metals, n.d.). To evaluate mechanical qualities without boundary influence, ISO13314 states that there must be enough unit cells in each direction. According to standards (Benedetti et al., 2021; Bobbert et al., 2017a; du Plessis et al., 2022a), compression tests require ten-unit cells in each direction. The presence of 10*10*10-unit cells in a 20mm test sample results in a unit cell of 2mm, which, even at 20% density, approaches a very tiny structure as the numerous wall thicknesses merge. As a result, researchers have shown that having fewer number unit

cells of about 5-7 cells in each direction leads to convergence of mechanical properties to a constant value (Ashby, 2000).

Different cellular structures, bulk material, densities, number of cells, cell orientation, cell size, wall thickness, and post-processing such as heat treatment define the final mechanical property of an additively manufactured lattice structure (Ashby, 2005a; Miralbes et al., 2020). For lattice structures, words like elastic modulus, yield strength, fatigue strength, and energy absorption are utilized. However, it has a different meaning for continuous materials; when referring to lattice structures, "as the number of unit cells gets large, the apparent macroscopic attributes of structures converge to a certain value" (Han et al., 2015).

The mechanical property of lattice structure depends majorly on relative density (λ) (Eq. (9)) which is defined by a power law (Eq. (10) and (11)), Gibson and Ashby's model relates the relative densities of cellular structures to their respective strength or modulus (Sharma and Hiremath, 2021). It is observed that as the λ decreases the lattice strength also decreases irrespective of lattice topology.

$$\lambda = \frac{\rho^*}{\rho^s} \qquad \text{... (9)}$$

$$\frac{\sigma^*}{\sigma^s} = C\left(\frac{\rho^*}{\rho^s}\right)^n \qquad \text{... (10)}$$

$$\frac{E^*}{E^s} = C\left(\frac{\rho^*}{\rho^s}\right)^n \qquad \text{... (11)}$$

Where ρ^*, σ^*, E^* are strength, modulus, and density of lattice structure ρ^s, σ^s, E^s and are strength, modulus density of base material. The coefficient 'C' is derived from experimental results and exponent value 'n' depends on mechanical response, that is, whether the structure is dominated by bending or by the stretch (Paufler, 1990).

Fig.6 represents the stress-strain curve under compression loading, in Fig.6. (a) graph displays gyroid TPMS samples evaluated at 12.5 per cent density, with an elastic zone followed by yielding at 20 MPa, then a plateau region with practically constant stress at 15 MPa, progressing to high stress and full densification. In Fig.6. (b) the graph depicts an experimental stress-strain curve using examples of skeleton gyroid constructions of differing densities (50 per cent, 37.5 per cent, 25 per cent, 12.5 per cent). As a result, it is obvious that as density drops, so does yield strength (du Plessis et al., 2022b).

The deformation of TPMS lattice for compressive strength is divided into three regions, as shown in the Fig.7. The first region is elastic where the curve is linear followed by the second region which is plastic, where the stress plateau is observed. Here plastic deformation occurs at an almost constant value of stress leading to breakage of the lattice structure, as a result, high energy absorption is observed in this particular region leading to the third region which is
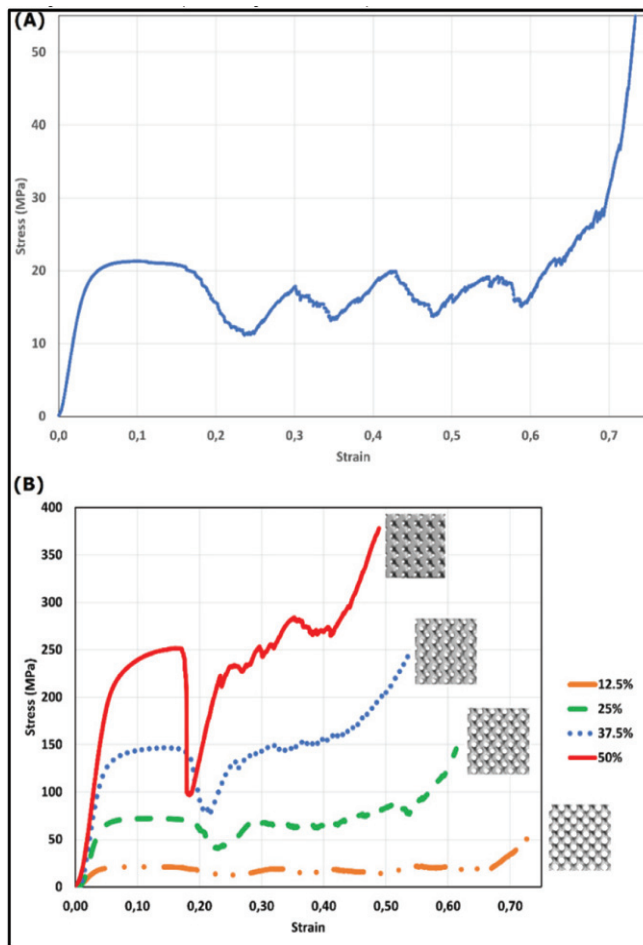
Figure 6: (A) Stress-strain curve for compression testing at 12.5 per cent density gyroid structure. (B) Compression testing stress-strain curve for gyroid structure with varying density (du Plessis et al., 2022b)
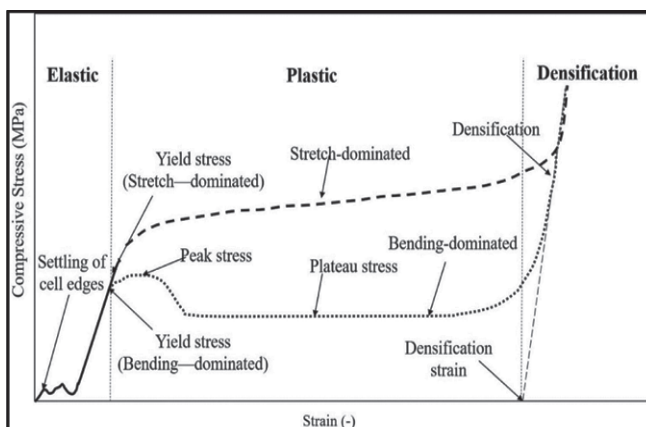

Figure 7: Compression behaviour of stretch and bending dominated structure in elastic, plastic and densification region

densification where the sample is crushed and it acts as a solid sample leading to higher values of stress (Khan et al., 2019).

Figure 7 illustrates that when opposed to bending-dominated structures, stretched-dominated structures have higher yield stress. However, bending-dominated structures are best suited for energy absorption applications because their plateau area is more stable (Rashed et al., 2016). Figure 8 depicts stress-strain curves under compression for primitive, gyroid, and diamond TPMS at various relative densities. Figure 9 depicts their experimental deformations as well. For primitive structures, there is a sharp increase in stress following the elastic zone and variability in stress in the plateau region, whereas the curves for gyroid and diamond are very smooth (Ashby, 2005b).

Figure 7 illustrates that when opposed to bending-dominated structures, stretched-dominated structures have higher yield stress. However, bending-dominated structures are best suited for energy absorption applications because their plateau area is more stable (Rashed et al., 2016). Figure 8 depicts stress-strain curves under compression for primitive, gyroid, and diamond TPMS at various relative densities. Figure 9 depicts their experimental deformations as well. For primitive structures, there is a sharp increase in stress following the elastic zone and variability in stress in the plateau region, whereas the curves for gyroid and diamond are very smooth (Ashby, 2005b).

The stress-strain curves for tensile strength testing are divided into 2 regions: elastic and brittle fracture. In general, lattice structures are loaded under compression and bend, resulting in local tensile stress (Bobbert et al., 2017b). Table I shows the tensile test results of Neovius and IWP structures when unit cell size, relative density, and average wall thickness were varied (Park et al., 2021).When unit cell size, wall thickness, and relative density are all reduced together, yield strength, tensile strength, and elastic modulus tend to increase, because lower unit cell size and average wall thickness also contribute to strength.

4.0 Methods and Materials for Additive Manufacturing and their Challenges

ASTM F2792-12 divides AM into seven processes: binder jetting, directed energy deposition, material extrusion, material netting, powder bed fusion, sheet lamination, and vat photopolymerization, with each method having its own precursor material, advantages, disadvantages, and applications (Standard Terminology for Additive Manufacturing Technologies, n.d.). Because Selective Laser Sintering (SLS) and Fused Deposition Modelling (FDM) are
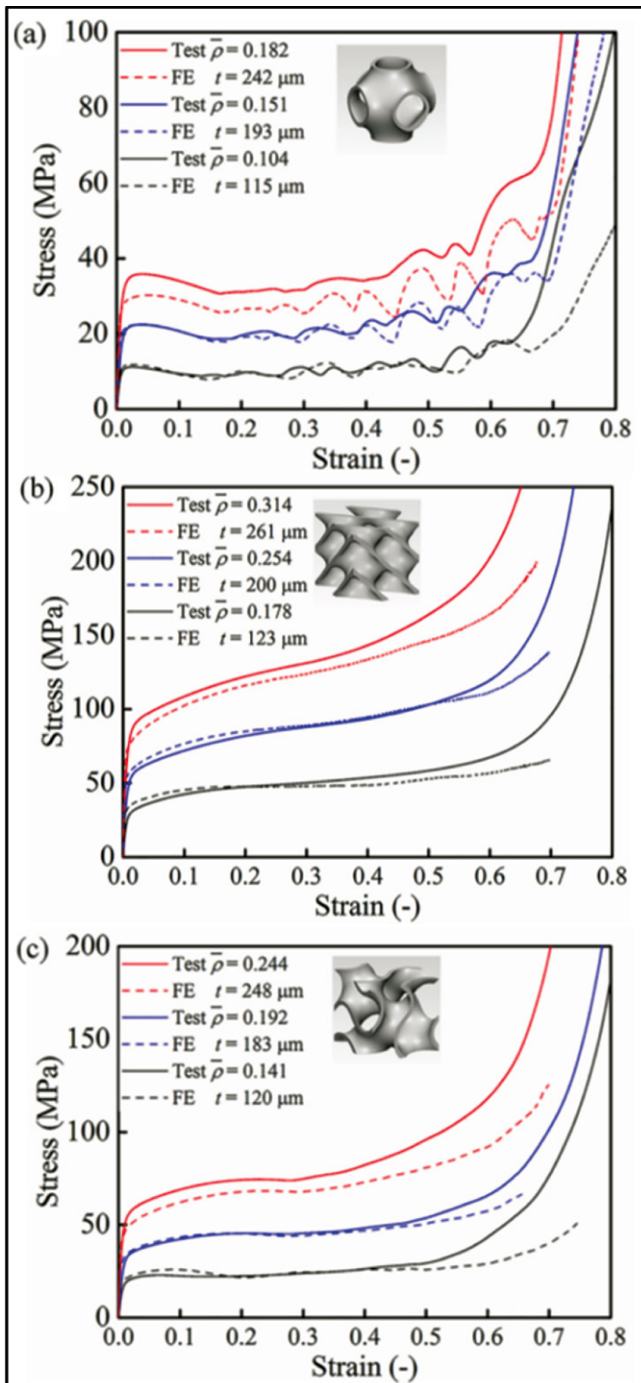
Figure 8: Experimental and numerical stress-strain curve (a) primitive, (b) diamond, (c) gyroid sheet structures (Feng Lu et al., 2018)

Figure 9: Experimental deformations of TPMS sheet structures. Arrows indicate failed layers (Feng Lu et al., 2018)

and is based on the principles of powder bed fusion and direct energy deposition. SLS benefits include exceptional dimensional accuracy, surface finish, and a rapid rate of deposition; thus, it is used in design prototypes and structural components of aircraft and satellites (Mohamed et al., 2017; Schmidt et al., 2017). FDM operates on the material extrusion concept and employs thermoplastics, ceramics, and polymers combined with metal particles as working materials in the form of a filament or paste. The fundamental advantage of this technology is the integration of diverse materials, which provides a higher degree of geometric independence. Although the need for post-processing and anisotropic material properties in parts are some of its limitations, this approach has applications in aerospace, automobiles, and 3D printed electronics (Multi-Jet Fluid Deposition In 3D Printing: A Review, n.d.; Travitzky et al., 2014).

A. Process Parameters and Challenges of SLS Technology

Many research and review publications focus on metal additive manufacturing cellular structures for which the SLS process is the most often employed approach. SLS is one of the oldest technologies developed and patented by CARL DECKARD in 1989. SLS uses powder as starting material and a laser as a heat source to bond the particles at the surface. "The powder bed is heated in the SLS process to avoid deformation and speed up bonding between the preceding layer and the layers that have been laid down. A laser is

the two most commonly used and popular technologies, they have been briefly discussed below.

SLS is a laser-based AM method that uses polymers, ceramics, and metals as working materials in a powder state
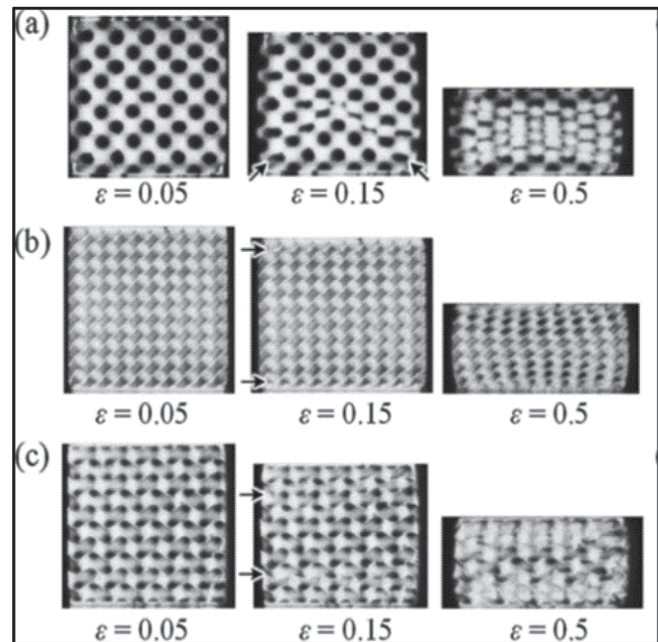
Table 1: Tensile properties of TPMS sheet lattice (Park et al., 2021)

Unit cell topology	Unit cell size, l, (mm)	Relative density, λ (%)	Average wall thickness, t (mm)	Tensile strength (MPa)	Elastic modulus (GPa)	Yield strength (MPa)
Neovius	1	73.6 ± 2.1	0.14 ± 0.01	34.4 ± 4.1	4.4 ± 0.1	25.0 ± 2.2
Neovius	2.5	28.1 ± 1.2	0.18 ± 0.02	62.2 ± 5.5	5.6 ± 0.7	33.5 ± 2.9
Neovius	5	17.8 ± 0.1	0.26 ± 0.02	381.2 ± 4.7	28.6 ± 0.1	242.6 ± 9.3
IWP	1	59.3 ± 2.5	0.14 ± 0.03	10.6 ± 5.4	1.0 ± 0.6	5.4 ± 2.3
IWP	2.5	25.5 ± 0.9	0.15 ± 0.02	38.4 ± 1.1	3.1 ± 0.5	25.1 ± 6.1
IWP	5	11.4 ± 0.2	0.14 ± 0.02	176.4 ± 11.6	14.5 ± 0.1	126.3 ± 6.1

Table 2 : Various parametrs of SLS technique for manufacturing TPMS structures

Machine	Material		Inert gas	Avg. practicle size (mm)	Layer thickness (μm)	Laser power (w)	Laser scanning rate (mm/s)	Powder bed tempera-ture e(□c)	Reference
MCP HEK realizer laser system	Metal	CoCrMo alloy powder	-	~30	30	90	376	-	(Park et al., 2021)
BLT-S210 system	Metal	316 stainless steel	Argon	15-53	20	-	1000	-	(X. Wang et al., 2020)
EOS p100	Polyamide	Pa 2200, nylon-12 based	-	35, 54, 82	100	21	2500	173	(X. Wang et al., 2020)
Formiga P100	Polyamide	Pa2200	-	56	100	30	-	172.5	(Abueidda et al., 2019)
Formiga P100	Polyamide	Pa2200	-	45	100	30	-	172.5	(Abueidda et al., 2017)
Formiga P100	Polyamide	Pa1102	-	50	80	21	2500	170	(Abou-Ali et al., 2020)

"-" indicates the absence of data

carefully steered over the particle layer in a predetermined route to sinter the particles, resulting in a solid layer. The platform is then lowered by the thickness of the layer, and a new layer of powder is rolled over the sintered layer. The unsintered powder remains in place and supports the overhanging component qualities. After the sintering process is repeated, the part is created" (Rapid Prototyping - Selective Laser Sintering (SLS), n.d.)

Major factors associated with the density and strength of SLS parts are particle size and distribution (Utela et al., 2008). It has been observed that laser scanning strategies contribute to the thermomechanical properties of the build path hence optimizing these scanning strategies can yield better control over the properties of the parts, also raster scanning path, laser exposure time, point distance, the density of the material, surface microstructure and roughness of the material

contribute to the final properties of the build. Hence while fabrication these variables must be controlled to get desired properties (Pham and Dimov, 2001). Table 2 lists the machines, materials, working environment, and regulating factors of the SLS technique for manufacturing TPMS structural components.

Suboptimal processing settings, porosity due to insufficient input energy, laser scanning method, and the staircase effect can all cause defects in the SLS process. Residual stress is caused by a significant temperature differential and can result in cracks, layer delamination, and geometrical defects as a result of shrinking (Grasso and Colosimo, n.d.; Leary et al., 2018). Hence to overcome the challenges more importance must be given to design constraints, processing parameters, and post-processing. As it has been noticed, the proper heat treatment aids in the relief

of thermal strains caused by the manufacturing process's high cooling rate (Echeta et al., 2019; Riemer et al., 2014).

5.0 Applications of TPMS

Because of the lightweight and high-strength nature of TPMS structures, they have sparked a lot of interest in the fields of engineering and medical science. While sports and safety equipment have begun to investigate the benefits of TPMS, biomedical and aerospace are two industries that have heavily invested and developed TPMS designs to monetize their benefits (Brennan-Craddock et al., 2012; Guo and Leu, 2013b).

A. Biomedicals

The medical implant market is presently worth 16 billion dollars and is predicted to reach 147 billion dollars by 2027 (Medical Implants Market Size | Industry Forecast by 2027, n.d.). The ability to manufacture high-quality metallic implants that so closely replicate the features of human bone in terms of strength, stiffness, density, weight, size, shape, and structure for a particular individual makes it such a huge industry. As a result, biomedical industries have shown interest in developing SLS technology and complex designs for TPMS structures(Barba et al., 2019).

Beyond the manufacturing of implants, some researchers have developed technology that stores drugs in the lattice structure cavity as a reservoir which is then locally released into the body(Burton et al., 2019).

B. Automobile

Low weight, high strength, and high heat transfer are something on which the aerospace industry has concentrated from the very beginning. With the continued development of AM techniques, partial goals of aerospace were achieved, further when TPMS structures was explode it showed that it solved all the major problems of the industry (Infinite Periodic Minimal Surfaces without Self-Intersections - NASA Technical Reports Server (NTRS), n.d.-a). These structures are lightweight and inspired by nature they have a continuous surface and also continuous voids which result in a cooling channel for heat transfer. Some researchers (Zhou et al., 2004) have developed and lattice structure-based thermal controller which increases the thermal capacity by 50% compared to the traditional thermal controller of similar mass.

6.0 Conclusions

This article presents an overview of the various characteristics of TPMS cellular structures, such as TPMS classification, types, governing equations, mechanical properties, failure modes, manufacturing processes, and applications. The following are some key points that may be drawn from the article:

- TPMS are inspired by nature and then mathematically modelled to manage the unit cell shape, size, relative density, and wall thickness in order to achieve a high-strength structure.
- These characteristics are directly related to the structure's strength. However, varying the quantities may produce intriguing outcomes.
- Processing and post-processing factors have a strong influence on the strength of structured components;thus, they must be carefully chosen.
- Although stretched dominated structures have a higher yield strength, bending dominated structures are preferable for energy absorption applications because to their stable plateau area.
- As gyroid and diamond TPMS structures feature a stable plateau zone, they are well suited for energy absorption applications.

This article aims to help readers understand TPMS structures and conduct their study.

7.0 Acknowledgement

Reference

1. Abou-Ali, A. M., Al-Ketan, O., Lee, D. W., Rowshan, R., & Abu Al-Rub, R. K. (2020). Mechanical behaviour of polymeric selective laser sintered ligament and sheet based lattices of triply periodic minimal surface architectures. *Materials & Design*, 196, 109100. https://doi.org/10.1016/J.MATDES.2020.109100
2. Abueidda, D. W., Bakir, M., Abu Al-Rub, R. K., Bergström, J. S., Sobh, N. A., & Jasiuk, I. (2017). Mechanical properties of 3D printed polymeric cellular materials with triply periodic minimal surface architectures. *Materials and Design*, 122, 255–267. https://doi.org/10.1016/J.MATDES.2017.03.018
3. Abueidda, D. W., Elhebeary, M., Shiang, C. S. (Andrew), Pang, S., Abu Al-Rub, R. K., & Jasiuk, I. M. (2019). Mechanical properties of 3D printed polymeric Gyroid cellular structures: Experimental and finite element study. *Materials & Design,* 165, 107597. https://doi.org/10.1016/J.MATDES.2019.107597
4. Al-Ketan, O., & Abu Al-Rub, R. K. (2019). Multifunctional Mechanical Metamaterials Based on

Triply Periodic Minimal Surface Lattices. *Advanced Engineering Materials*, 21(10), 1900524. https://doi.org/10.1002/ADEM.201900524

5. Al-Ketan, O., Rowshan, R., & Abu Al-Rub, R. K. (2018). Topology-mechanical property relationship of 3D printed strut, skeletal, and sheet based periodic metallic cellular materials. *Additive Manufacturing*, 19, 167–183. https://doi.org/10.1016/J.ADDMA.2017.12.006

6. Ashby, M. F. (2000). Metal foams/ : a design guide. 251.

7. Ashby, M. F. (2005a). The properties of foams and lattices. *Philosophical Transactions of the Royal Society A: Mathematical, Physical and Engineering Sciences,* 364(1838), 15–30. https://doi.org/10.1098/RSTA.2005.1678

8. Ashby, M. F. (2005b). The properties of foams and lattices. *Philosophical Transactions of the Royal Society A: Mathematical, Physical and Engineering Sciences*, 364(1838), 15–30. https://doi.org/10.1098/RSTA.2005.1678

9. Barba, D., Alabort, E., & Reed, R. C. (2019). Synthetic bone: Design by additive manufacturing. *Acta Biomaterialia*, 97, 637–656. https://doi.org/10.1016/J.ACTBIO.2019.07.049

10. Benedetti, M., du Plessis, A., Ritchie, R. O., Dallago, M., Razavi, S. M. J., & Berto, F. (2021). Architected cellular materials: A review on their mechanical properties towards fatigue-tolerant design and fabrication. Materials Science and Engineering: R: Reports, 144, 100606. https://doi.org/10.1016/*J. MSER.*2021.100606

11. Bobbert, F. S. L., Lietaert, K., Eftekhari, A. A., Pouran, B., Ahmadi, S. M., Weinans, H., & Zadpoor, A. A. (2017a). Additively manufactured metallic porous biomaterials based on minimal surfaces: A unique combination of topological, mechanical, and mass transport properties. *Acta Biomaterialia*, 53, 572–584. https://doi.org/10.1016/J.ACTBIO.2017.02.024

12. Bobbert, F. S. L., Lietaert, K., Eftekhari, A. A., Pouran, B., Ahmadi, S. M., Weinans, H., & Zadpoor, A. A. (2017b). Additively manufactured metallic porous biomaterials based on minimal surfaces: A unique combination of topological, mechanical, and mass transport properties. *Acta Biomaterialia*, 53, 572–584. https://doi.org/10.1016/J.ACTBIO.2017.02.024

13. Brennan-Craddock, J., Brackett, D., Wildman, R., & Hague, R. (2012). The design of impact absorbing structures for additive manufacture. *Journal of Physics: Conference Series,* 382(1). https://doi.org/10.1088/1742-6596/382/1/012042

14. Burton, H. E., Eisenstein, N. M., Lawless, B. M.,

Jamshidi, P., Segarra, M. A., Addison, O., Shepherd, D. E. T., Attallah, M. M., Grover, L. M., & Cox, S. C. (2019). The design of additively manufactured lattices to increase the functionality of medical implants. Materials Science & Engineering. C, Materials for Biological Applications, 94, 901–908. https://doi.org/10.1016/J.MSEC.2018.10.052

15. Chen, H., Han, Q., Wang, C., Liu, Y., Chen, B., & Wang, J. (2020). Porous Scaffold Design for Additive Manufacturing in Orthopedics: A Review. Frontiers in Bioengineering and Biotechnology, 8, 609. https://doi.org/10.3389/FBIOE.2020.00609/BIBTEX

16. Chen, H. Y., Kwon, Y., & Thornton, K. (2009). Multifunctionality of three-dimensional self-assembled composite structure. Scripta Materialia, 1(61), 52–55. https://doi.org/10.1016/J.SCRIPTAMAT.2009.03.006

17. du Plessis, A., Razavi, S. M. J., Benedetti, M., Murchio, S., Leary, M., Watson, M., Bhate, D., & Berto, F. (2022a). Properties and applications of additively manufactured metallic cellular materials: A review. *Progress in Materials Science,* 125, 100918. https://doi.org/10.1016/J.PMATSCI.2021.100918

18. du Plessis, A., Razavi, S. M. J., Benedetti, M., Murchio, S., Leary, M., Watson, M., Bhate, D., & Berto, F. (2022b). Properties and applications of additively manufactured metallic cellular materials: A review. *Progress in Materials Science*, 125, 100918. https://doi.org/10.1016/J.PMATSCI.2021.100918

19. Echeta, I., Feng, X., Dutton, B., Leach, R., & Piano, S. (2019). Review of defects in lattice structures manufactured by powder bed fusion. The International *Journal of Advanced Manufacturing Technology 2019* 106:5, 106(5), 2649–2668. https://doi.org/10.1007/S00170-019-04753-4

20. Feng Lu, W., Zhang, L., Feih, S., Daynes, S., Chang, S., Yu Wang, M., & Wei, J. (2018). Energy absorption characteristics of metallic triply periodic minimal surface sheet structures under compressive loading. 23, 505–515.

21. Frazier, W. E. (2014). Metal additive manufacturing: A review. *Journal of Materials Engineering and Performance*, 23(6), 1917–1928. https://doi.org/10.1007/S11665-014-0958-Z/FIGURES/9

22. Gandy, P. J. F., & Klinowski, J. (2002). Nodal Surface Approximations to the Zero Equipotential Surfaces for Cubic Lattices. *Journal of Mathematical Chemistry 2002* 31:1, 31(1), 1–16. https://doi.org/10.1023/A:1015444012997

23. Grasso, M., & Colosimo, B. M. (n.d.). Process defects and in situ monitoring methods in metal powder bed fusion: A review Grasso, MARCO LUIGI; Colosimo, BIANCA MARIA Process Defects and In-situ

Monitoring Methods in Metal Powder Bed Fusion: a Review. https://doi.org/10.1088/1361-6501/aa5c4f

24. Guo, N., & Leu, M. C. (2013a). Additive manufacturing: Technology, applications and research needs. *Frontiers of Mechanical Engineering*, 8(3), 215–243. https://doi.org/10.1007/S11465-013-0248-8

25. Guo, N., & Leu, M. C. (2013b). Additive manufacturing: Technology, applications and research needs. *Frontiers of Mechanical Engineering*, 8(3), 215–243. https://doi.org/10.1007/S11465-013-0248-8

26. Han, S. C., Lee, J. W., & Kang, K. (2015). A New Type of Low Density Material: Shellular. *Advanced Materials*, 27(37), 5506–5511. https://doi.org/10.1002/ADMA.201501546

27. Infinite periodic minimal surfaces without self-intersections - NASA Technical Reports Server (NTRS). (n.d.-a). Retrieved May 10, 2022, from https://ntrs.nasa.gov/citations/19700020472

28. Infinite periodic minimal surfaces without self-intersections - NASA Technical Reports Server (NTRS). (n.d.-b). Retrieved May 10, 2022, from https://ntrs.nasa.gov/citations/19700020472

29. ISO - ISO 13314:2011 - Mechanical testing of metals – Ductility testing – Compression test for porous and cellular metals. (n.d.). Retrieved May 10, 2022, from https://www.iso.org/standard/53669.html

30. Khan, S. Z., Masood, S. H., Ibrahim, E., & Ahmad, Z. (2019). Compressive behaviour of Neovius Triply Periodic Minimal Surface cellular structure manufactured by fused deposition modelling. Https://Doi.Org/10.1080/17452759.2019.1615750, 14(4), 360–370. https://doi.org/10.1080/17452759.2019.1615750

31. Lai, M., Kulak, A. N., Law, D., Zhang, Z., Meldrum, F. C., & Riley, D. J. (2007). Profiting from nature: macroporous copper with superior mechanical properties. Chemical Communications, 34, 3547–3549. https://doi.org/10.1039/B707469G

32. Leary, M., Mazur, M., Williams, H., Yang, E., Alghamdi, A., Lozanovski, B., Zhang, X., Shidid, D., Farahbod-Sternahl, L., Witt, G., Kelbassa, I., Choong, P., Qian, M., & Brandt, M. (2018). Inconel 625 lattice structures manufactured by selective laser melting (SLM): Mechanical properties, deformation and failure modes. *Materials and Design*, 157, 179–199. https://doi.org/10.1016/J.MATDES.2018.06.010

33. Medical Implants Market Size | Industry Forecast by 2027. (n.d.). Retrieved May 10, 2022, from https://www.alliedmarketresearch.com/medical-implants-market

34. Miralbes, R., Ranz, D., Pascual, F. J., Zouzias, D., & Maza, M. (2020). Characterization of additively manufactured triply periodic minimal surface structures under compressive loading. Https://Doi.Org/10.1080/15376494.2020.1842948. https://doi.org/10.1080/15376494.2020.1842948

35. Mohamed, O. A., Masood, S. H., & Bhowmik, J. L. (2017). Experimental investigation of time-dependent mechanical properties of PC-ABS prototypes processed by FDM additive manufacturing process. *Materials Letters*, C(193), 58–62. https://doi.org/10.1016/J.MATLET.2017.01.104

36. Multi-Jet Fluid Deposition In 3D Printing: A Review. (n.d.). Retrieved May 10, 2022, from https://www.jetir.org/view?paper=JETIRA006021

37. Park, S. Y., Kim, K. S., AlMangour, B., Grzesiak, D., & Lee, K. A. (2021). Effect of unit cell topology on the tensile loading responses of additive manufactured CoCrMo triply periodic minimal surface sheet lattices. Materials & Design, 206, 109778. https://doi.org/10.1016/J.MATDES.2021.109778

38. Paufler, P. (1990). L. L. Gibson, M. F. Ashby. Cellular solids. Structure & properties. Pergamon Press, Oxford 1988. IX + 357 p. Preis $ 40.00. ISBN 0-08-036607-4. *Crystal Research and Technology*, 25(9), 1038–1038. https://doi.org/10.1002/CRAT.2170250912

39. Pham, D. T., & Dimov, S. S. (2001). Rapid Manufacturing. https://doi.org/10.1007/978-1-4471-0703-3

40. Poladian, L., Wickham, S., Lee, K., & Large, M. C. J. (2008). Iridescence from photonic crystals and its suppression in butterfly scales. J*ournal of The Royal Society Interface*, 6(SUPPL. 2). https://doi.org/10.1098/RSIF.2008.0353.FOCUS

41. Rapid Prototyping - Selective Laser Sintering (SLS). (n.d.). Retrieved May 10, 2022, from https://www.custompartnet.com/wu/selective-laser-sintering

42. Rashed, M. G., Ashraf, M., Mines, R. A. W., & Hazell, P. J. (2016). Metallic microlattice materials: A current state of the art on manufacturing, mechanical properties and applications. *Materials and Design*, 95, 518–533. https://doi.org/10.1016/J.MATDES.2016.01.146

43. Riemer, A., Leuders, S., Thöne, M., Richard, H. A., Tröster, T., & Niendorf, T. (2014). On the fatigue crack growth behaviour in 316L stainless steel manufactured by selective laser melting. *Engineering Fracture Mechanics,* 120, 15–25. https://doi.org/10.1016/J.ENGFRACMECH.2014.03.008

44. Schmidt, M., Merklein, M., Bourell, D., Dimitrov, D., Hausotte, T., Wegener, K., Overmeyer, L., Vollertsen, F., & Levy, G. N. (2017). Laser based additive manufacturing in industry and academia. CIRP Annals - *Manufacturing Technology,* 2(66), 561–583. https://doi.org/10.1016/J.CIRP.2017.05.011

45. Schwarz, H. A. 1843-1921. (2005). Gesammelte mathematische Abhandlungen, von H. A. Schwarz. http://name.umdl.umich.edu/AAT0607.0001.001

46. Sharma, D., & Hiremath, S. S. (2021). Additively manufactured mechanical metamaterials based on triply periodic minimal surfaces: Performance, challenges, and application. Https://Doi.Org/10.1080/15376494.2021.1948151. https://doi.org/10.1080/15376494.2021.1948151

47. Standard Terminology for Additive Manufacturing Technologies,. (n.d.). Retrieved May 10, 2022, from https://www.astm.org/f2792-12.html

48. Tafazoli, M., & Nouri, M. D. (2020). Investigation of the experimental, statistical and optimisation of 3D printed lattice core sandwich panel energy absorber with novel configuration using response surface method. Https://Doi.Org/10.1080/13588265.2020.1786913, 1–12. https://doi.org/10.1080/13588265.2020.1786913

49. Torquato, S., & Donev, A. (2004). Minimal surfaces and multifunctionality. Proceedings of the Royal Society A: Mathematical, Physical and Engineering Sciences, 460(2047), 1849–1856. https://doi.org/10.1098/RSPA.2003.1269

50. Travitzky, N., Bonet, A., Dermeik, B., Fey, T., Filbert-Demut, I., Schlier, L., Schlordt, T., & Greil, P. (2014). Additive Manufacturing of Ceramic-Based Materials. *Advanced Engineering Materials,* 16(6), 729–754.

https://doi.org/10.1002/ADEM.201400097

51. Utela, B., Storti, D., Anderson, R., & Ganter, M. (2008). A review of process development steps for new material systems in three dimensional printing (3DP). *Journal of Manufacturing Processes*, 10, 96–104. https://doi.org/10.1016/j.jmapro.2009.03.002

52. Wang, L., Lau, J., Thomas, E. L., & Boyce, M. C. (2011). Co-Continuous Composite Materials for Stiffness, Strength, and Energy Dissipation. *Advanced Materials*, 23(13), 1524–1529. https://doi.org/10.1002/ADMA.201003956

53. Wang, X., Wang, C., Zhou, X., Zhang, M., Zhang, P., & Wang, L. (2020). Innovative design and additive manufacturing of regenerative cooling thermal protection system based on the triply periodic minimal surface porous structure. CMES - Computer Modeling in Engineering and Sciences, 123(2), 495–508. https://doi.org/10.32604/CMES.2020.09778

54. Yan, C., Hao, L., Hussein, A., Young, P., & Raymont, D. (2014). Advanced lightweight 316L stainless steel cellular lattice structures fabricated via selective laser melting. *Materials and Design*, 55, 533–541. https://doi.org/10.1016/J.MATDES.2013.10.027

55. Zhou, J., Shrotriya, P., & Soboyejo, W. O. (2004). On the deformation of aluminum lattice block structures: from struts to structures. *Mechanics of Materials*, 36(8), 723–737. https://doi.org/10.1016/J.MECHMAT.2003.08.007